frontiers | Frontiers in Bioengineering and Biotechnology

ORIGINAL RESEARCH
published: 02 May 2022
doi: 10.3389/fbioe.2022.889717

Effects of Bacterial Culture and Calcium Source Addition on Lead and Copper Remediation Using Bioinspired Calcium Carbonate Precipitation

Zhong-Fei Xue[1,2], *Wen-Chieh Cheng*[1,2]*, *Lin Wang*[1,2] *and Shaojie Wen*[1,2]

[1]School of Civil Engineering, Xi'an University of Architecture and Technology, Xi'an, China, [2]Shaanxi Key Laboratory of Geotechnical and Underground Space Engineering (XAUAT), Xi'an, China

Lead and copper ions from wastewater induced by metallurgical processes are accumulated in soils, threatening plant and human health. The bioinspired calcium carbonate precipitation is proven effective in improving the cementation between soil particles. However, studies on capsulizing heavy metal ions using the bioinspired calcium carbonate precipitation are remarkably limited. The present study conducted a series of test tube experiments to investigate the effects of bacterial culture and calcium source addition on the remediation efficiency against lead and copper ions. The calcium carbonate precipitation was reproduced using the Visual MINTEQ software package to reveal the mechanism affecting the remediation efficiency. The degradation in the remediation efficiency against lead ions relies mainly upon the degree of urea hydrolysis. However, higher degrees of urea hydrolysis cause remediation efficiency against copper ions to reduce to zero. Such high degree of urea hydrolysis turns pH surrounding conditions into highly alkaline environments. Therefore, pursuing higher degrees of urea hydrolysis might not be the most crucial factor while remedying copper ions. The findings shed light on the importance of modifying pH surrounding conditions in capsulizing copper ions using the bioinspired calcium carbonate precipitation.

Keywords: bioinspired calcium carbonate precipitation, *Sporosarcina pasteurii*, pH, urea hydrolysis, remediation efficiency

OPEN ACCESS

Edited by:
Ming Xie,
University of Bath, United Kingdom

Reviewed by:
Jinchen Fan,
University of Shanghai for Science and Technology, China
Hao Peng,
Yangtze Normal University, China

***Correspondence:**
Wen-Chieh Cheng
w-c.cheng@xauat.edu.cn

Specialty section:
This article was submitted to Bioprocess Engineering, a section of the journal Frontiers in Bioengineering and Biotechnology

Received: *04 March 2022*
Accepted: *30 March 2022*
Published: *02 May 2022*

Citation:
Xue Z-F, Cheng W-C, Wang L and Wen S (2022) Effects of Bacterial Culture and Calcium Source Addition on Lead and Copper Remediation Using Bioinspired Calcium Carbonate Precipitation. Front. Bioeng. Biotechnol. 10:889717. doi: 10.3389/fbioe.2022.889717

INTRODUCTION

Metallurgical processes, metal smelting activities, and inappropriate wastewater disposal discharge heavy metals into soils and groundwater, hence resulting in serious ecological environmental pollution (Nakata et al., 2017; Vital et al., 2018; Bai et al., 2021a; Bai et al., 2021b; Bai et al., 2021d; Xue et al., 2021a; Xue et al., 2021b; Wang et al., 2021; Chen et al., 2022). Lead (Pb) and copper (Cu), that are featured with characters of toxicity, non-biodegradability, and bioaccumulation, are considered two common and dangerous heavy metal contaminants present in surrounding environments, which cause serious threats to plant and human health (Zhao et al., 2016; Jiang et al., 2019; Liao et al., 2020). The mobility or solubility of heavy metals can transform them from the solid phase to the solution phase, thereby increasing their bioavailability (Bolan et al., 2014; Bai et al., 2020, Bai et al., 2021c; Yang et al., 2021; Xue et al., 2022). Therefore, immobilizing heavy metals is

considered to be of great necessity in order to reduce their bioavailability (Li et al., 2013; Khadim et al., 2019; Cheng et al., 2021; Hu et al., 2021; Hu et al., 2022; Wang et al., 2022; Wang et al., 2022; Wang et al., 2022). To this end, chemical precipitation, electroremediation, and ion-exchange and adsorption have been widely adopted as countermeasures. Notwithstanding that, these methods are neither effective nor economical and may cause secondary environmental contamination (Bhattacharya et al., 2018; Zhao et al., 2020). Bioprecipitation of calcium carbonate has recently gained much attention from scientific researchers and industrial participants, which is proven economic and effective for immobilizing heavy metals and substantially reduces the potential of secondary environmental contamination (Rahman et al., 2020; Rajasekar et al., 2021).

The fundamental principle of applying the bioinspired calcium carbonate precipitation technology to the immobilization of heavy metals is to catalyze urea hydrolysis using the ureolytic bacteria toward discharging hydroxide ions and ammonium ions and precipitating calcium carbonate with heavy metals (Schwantes-Cezario et al., 2017; Qiao et al., 2019; Schwantes-Cezario et al., 2020; Yang et al., 2020; Hu et al., 2021a; Hu et al., 2021b; Yuyang Zhang et al., 2021; Yuan et al., 2021). The whole process is also referred to as "biomineralization", and heavy metal migration potential can be substantially reduced when capsulized using the calcium carbonate precipitation, minimizing their threats to surrounding environments (Zhu and Maria, 2016; Arias et al., 2019; Teng et al., 2019; Song et al., 2021) (see **Eqs 1–7**). Jiang et al. (2019) reported that calcium source and bacterial concentration can affect the remediation efficiency against lead and three mechanisms, namely, abiotic precipitation, biotic precipitation, and biosorption, which take part in the biomineralization process. Qiao et al., 2021 declared that the bioinspired calcium carbonate precipitation technology is effective in removing heavy metals such as Cu, Zn, Ni, and Cd.

$$CO(NH_2)_2 + H_2O \rightarrow 2NH_3 + CO_2. \quad (1)$$

$$2NH_3 + 2H_2O \leftrightarrow 2NH_4^+ + 2OH^-. \quad (2)$$

$$CO_2 + 2OH \leftrightarrow HCO_3^- + OH^- \leftrightarrow CO_3^{2-} + H_2O. \quad (3)$$

$$Ca^{2+} + Cell \rightarrow Cell - Ca^{2+}. \quad (4)$$

$$M^{2+} + Cell \rightarrow Cell - M^{2+}. \quad (5)$$

$$Cell - Ca^{2+} + CO_3^{2-} \rightarrow Cell - CaCO_3(s). \quad (6)$$

$$Cell - M^{2+} + CO_3^{2-} \rightarrow Cell - MCO_3(s). \quad (7)$$

A ratio of the removed heavy metal concentration to the initial concentration has been defined as remediation efficiency, and it may vary with the degree of urea hydrolysis, pH surrounding conditions, and concentration of heavy metal ions (Achal et al., 2012; Xue et al., 2022). As reported by Duarte-Nass et al. (2020), the remediation efficiency against copper degrades with the decrease in the degree of urea hydrolysis, and the degradation becomes more pronounced when subjected to higher heavy metal concentrations. Mugwar and Harbottle (2016) found that elevation of pH surrounding conditions and calcium carbonate precipitation is shown to be strongly linked to the removal of zinc and cadmium. Although a significant body of research has investigated the degree of urea hydrolysis and its link to remediation efficiency, how they vary with the effect of bacterial culture remains unclear (Torres-Aravena et al., 2018; Seplveda et al., 2021; Shi et al., 2022). Furthermore, given that calcium source addition takes part in precipitating calcium carbonate, its implications on the ureolytic bacteria and urease activity are, however, rarely studied. The main objectives of the present study are as follows: 1) to investigate the effect of bacterial culture and calcium source addition on the remediation efficiency against Pb^{2+} and Cu^{2+} and 2) to reveal the mechanism affecting remediation efficiency.

MATERIALS AND METHODS

Bacteria and Cultivation

Sporosarcina pasteurii in a freeze-dried form from China General Microbiological Culture Collection Center (CGMCC) was used as ureolytic bacteria for catalyzing urea hydrolysis. The strain was transferred to a liquid medium which consists of yeast extract (Oxoid Ltd., United Kingdom) of 20 g/L, urea (Damao Chemical Reagent Factory, China) of 20 g/L, NH_4Cl (Chengdu Chron Chemicals Co. Ltd., China) of 10 g/L, $MnSO_4{\cdot}H_2O$ (Shanghai Aladdin Biochemical Technology Co. Ltd., China) of 10 mg/L, and $NiCl{\cdot}6H_2O$ (Tianli Chemical Reagent Co. Ltd., China) of 24 mg/L and was cultured at 180 rpm and 30°C for 24 h. pH for the liquid medium was measured being 8.8. The activated ureolytic bacteria were mixed with glycerol using a ratio of 7:3 and stored at −20°C (Achal et al., 2012). They were used as the inoculum in subsequent test tube experiments.

Test Tube Experiments

The purpose for implementing the test tube experiments is to reproduce the biomineralization process using the ureolytic bacteria for Pb and Cu immobilization. The testing scheme for the test tube experiments under the effect of bacterial culture (i.e., yeast extract) and calcium source (i.e., $CaCl_2$) addition is summarized in **Table 1**. Bacterial solution from the frozen stock was first inoculated (0.1% (v/v)) into the liquid medium containing $Cu(NO_3)_2$ or $Pb(NO_3)_2$ at concentrations varying in a 0–50 mM range, 0.5 M urea, 2 g/L yeast extract, and 0.25 M $CaCl_2$. There were three replicates for each testing set. Urease activity (UA) and pH measurements were conducted at 0, 4, 12, 24, and 48 h, while NH_4^+ and Pb^{2+} or Cu^{2+} concentration were measured at 0, 24, and 48 h, respectively. pH was measured using a bench pH meter (Hanna Instruments Inc. HI 2003), while UA was measured on a basis of the ureolysis rate, as recommended by Whiffin et al. (2007); 2 ml reaction solution is mixed with 18 ml 1.11 M urea, and EC is measured at 0 and 5 min after mixing. UA can be evaluated using the equation below:

$$UA = \frac{EC_5 - EC_0}{5} \times 10 \times 1.11\,(\text{mM Urea min}^{-1}), \quad (8)$$

where EC_0 and EC_5 are electrical conductivity at 0 and 5 min, respectively. Furthermore, NH_4^+ concentration in solution was

TABLE 1 | Scheme applied to the test tube experiments.

	Bacterial inoculation proportion	Concentration of yeast extract (g/L)	Concentration of $CaCl_2$ (mM)	Concentration of $Cu(NO_3)_2$/$Pb(NO_3)_2$ (mM)
Exp-01	1:9	0	0	0, 5, 10, 20, 30, 40, and 50
Exp-02	1:9	20	0	
Exp-03	1:9	20	0.25	

TABLE 2 | Summary of the numerical simulations.

$CaCl_2$ (mM)	Concentration of each ions (mM)					
	Cu^{2+}/Pb^{2+}	NO_3^-	NH_4^+	CO_3^{2-}	Cl^-	Ca^{2+}
0	5, 10, 20, 30, 40, and 50	10, 20, 40, 60, 80, and 100	33.3–1,033.3	0–500	33.3	0
0.25					533.3	250

determined using the modified Nessler method (Whiffin et al., 2007). Moreover, Pb^{2+} or Cu^{2+} concentration was measured using an atomic spectrophotometer (Beijing Purkinje General Instrument TAS-990). The remediation efficiency can be evaluated as follows:

$$Remediation\ efficiency = \frac{C_1 - C_0}{C_0} \times 100\%, \quad (9)$$

where C_0 and C_1 are Pb^{2+} or Cu^{2+} concentration before and after remediation, respectively. NH_4^+ concentration of the reaction solution is measured at 0.1, 24, and 48 h, and the method for measuring NH_4^+ concentration corresponds to the modified Nessler method (Whiffin et al., 2007). Prior to the measurement, a calibration line was set up, and the absorbance was measured using a spectrophotometer 10 min after adding Nessler's reagent and potassium sodium tartrate. It was substituted into the calibration line, yielding NH_4^+ concentration. The more the NH_4^+ produced, the higher the degree of urea hydrolysis. For this reason, the NH_4^+ concentration was adopted here toward assessing the degree of urea hydrolysis.

Biomineralization Simulation

Given that the speciation and sequence of carbonate precipitation cannot be revealed by the experimental results, they were reproduced using the Visual MINTEQ software package. In the present work, urea hydrolysis was modeled using the ratio of NH_4^+ to CO_3^{2-} being 2:1, although the bacterial culture and inoculation were omitted in the numerical simulation (Gat et al., 2017). NH_4^+ and CO_3^{2-} concentrations that are extracted upon the completion of urea hydrolysis aim to backanalyze the speciation and sequence of carbonate precipitation. The details in terms of the numerical simulation are summarized in **Table 2**. The simulated results are beneficial to analyze how the speciation and sequence of carbonate precipitation vary under the sole effect of yeast extract and the effect of yeast extract and calcium source addition.

RESULTS AND DISCUSSION

Effect of Bacterial Culture and Calcium Source Addition

UA and pH are deemed as the key indicators that reflect the degree of urea hydrolysis and remediation efficiency while introducing the microbial-induced carbonate precipitation (MICP) technology for heavy metal immobilization (Stocks-Fischer et al., 1999; Zhu and Maria, 2016; Omoregie et al., 2017). This section aims to analyze the effect of bacterial culture and calcium source addition on the degree of urea hydrolysis during the MICP process. As shown in **Figures 1A–C**, UA generally decreases with the increase of $Pb(NO_3)_2$ concentration. The temporal relationships, when not subjected to yeast extract and $CaCl_2$ addition, can be characterized as UA ascending initially and descending after reaching the peak (**Figure 1A**). Furthermore, the temporal relationships of UA are divided into two curve groups; the temporal relationships of UA under the $Pb(NO_3)_2$ concentration ≤20 mM lie above those under the $Pb(NO_3)_2$ concentration >20 Mm. When subjected to the effect of yeast extract, the temporal relationships of UA are found to occur in an ascending manner throughout (**Figure 1B**). The temporal relationships under the effect of yeast extract and $CaCl_2$ addition can be characterized as UA descending initially and ascending after reaching the minimum value (**Figure 1C**).

The secretion of urease by the ureolytic bacteria is determined by whether the availability of sufficient nutrients can be assured for bacterial growth and reproduction. Higher concentrations of Pb^{2+} prevent the ureolytic bacteria from secreting and producing enough extracellular polysaccharides (EPS), aggravating the effect of Pb^{2+} and deactivating the ureolytic bacteria (Wu et al., 2019). On the other hand, higher Pb^{2+} concentrations can also cause urease denaturation, leading to its deactivation. These results, in turn, impede the development of UA. The consumption of nutrients over time is the main contributor to the formation of the descending tendency of bacterial activity. For this reason, UA descends slowly after 24 h (**Figure 1A**). In contrast, the

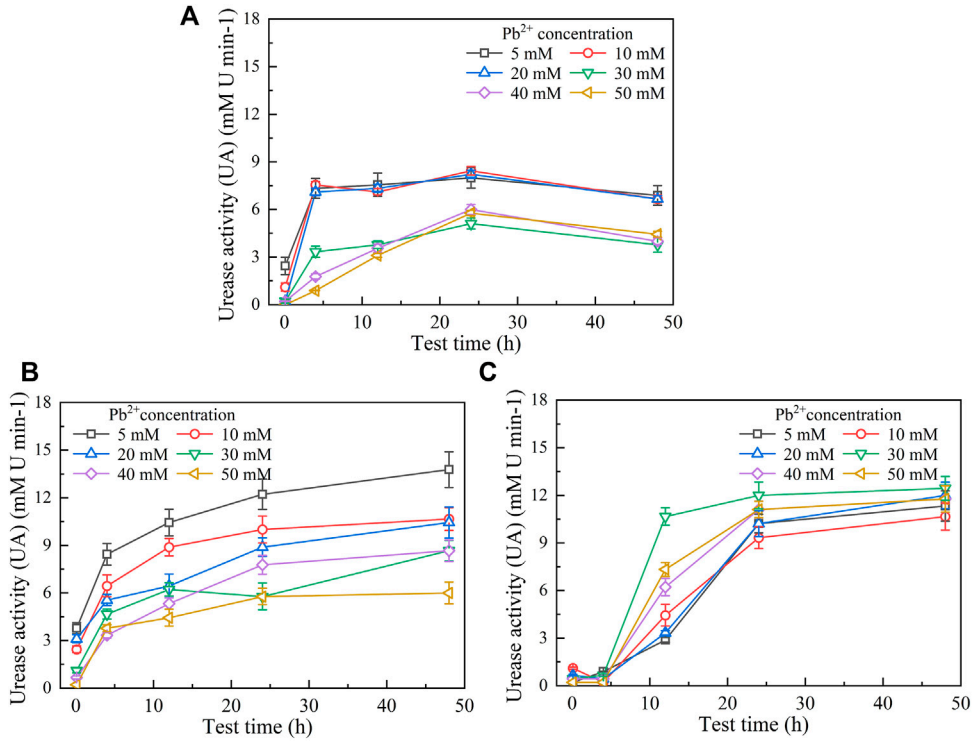

FIGURE 1 | Temporal relationships of urease activity (UA) against $Pb(NO_3)_2$ concentrations: **(A)** without yeast extract and $CaCl_2$ addition, **(B)** under the effect of yeast extract, and **(C)** under the effect of yeast extract and $CaCl_2$ addition.

ureolytic bacteria under the effect of yeast extract continuously secrete urease, and therefore, UA increases all along (**Figure 1B**). Considering $CaCl_2$ is a calcium source addition and the yeast extract aids the ureolytic bacteria to secrete urease, the negatively charged ureolytic bacteria adsorb Pb^{2+} and Ca^{2+} and precipitate with CO_3^{2-} when using the ureolytic bacteria as nucleation sites (Rui Zhang et al., 2021; Yin et al., 2021). To this end, the ureolytic bacteria settle together with the carbonate precipitation toward the bottom of the test tube, reducing the bacterial concentration in the supernatant and subsequently reducing UA (**Figure 1C**). Thus, UA shows a decreasing tendency from 0.1 to 4 h . Ca^{2+} form competitive adsorption with Pb^{2+} and cause the ureolytic bacteria to preferentially bind themselves together with Ca^{2+}, which also indicates an enhancement of the resistance against Pb^{2+}. Given the effect of $CaCl_2$ addition, the ureolytic bacteria that commence showing their resistance against the effect of Pb^{2+} continue to grow and secrete urease, and therefore, UA increases after reaching the minimum from 4 to 48 h. This shows a difference in the curve slopes from those we have seen in **Figure 1B**.

The temporal relationships of pH in the mixture against $Pb(NO_3)_2$ concentrations are shown in **Figure 2**. They can be characterized with the pH increasing rapidly at the very beginning of the MICP process and then remaining constant or decreasing slightly after reaching the peak. Furthermore, similar to the temporal relationships of UA, pH decreases with the increase of $Pb(NO_3)_2$ concentration. Moreover, when subjected to no yeast extract and $CaCl_2$ addition, pH reaches its maximum value being approximately 9.5 at 12 h after the commencement of the MICP process (**Figure 2A**). pH, when subjected to the effect of yeast extract, reaches its maximum of about 8.5 after 12 h, which is close to that under the effect of yeast extract and $CaCl_2$ addition (**Figures 2B,C**). These results can help infer that under the sole effect of yeast extract, a small number of ureolytic bacteria remain active when subjected to lower Pb^{2+} concentrations and the majority of the ureolytic bacteria lose their activity when subjected to higher Pb^{2+} concentrations. The smaller the number of ureolytic bacteria remaining active, the lower the degree of ureo hydrolysis. Therefore, UA distributes in a scattered manner at the end of the process, and due to the lack of NH_4^+ resulting from the reduced degree of urea hydrolysis, pH reduces to 8.5. pH reducing to 8.5 could also be ascribed to bacteria metabolism. Bacteria metabolism consumes carbon from the yeast extract, yielding organic and carbonic acids and lowering pH (Jimenez-Lopez et al., 2008). In contrast, UA is beyond 10 at the end of the process under the effect of yeast extract and $CaCl_2$ addition. This is because the majority of the ureolytic bacteria commence showing their resistance against the effect of Pb^{2+} (Peng et al., 2021). The higher degree of urea hydrolysis facilitates the formation of carbonate precipitation, which also indicates consumption of CO_3^{2-} and further decrease in pH.

Figures 3, 4 show the temporal relationships of UA and pH against $Cu(NO_3)_2$ concentrations, respectively. UA = 5 mM U

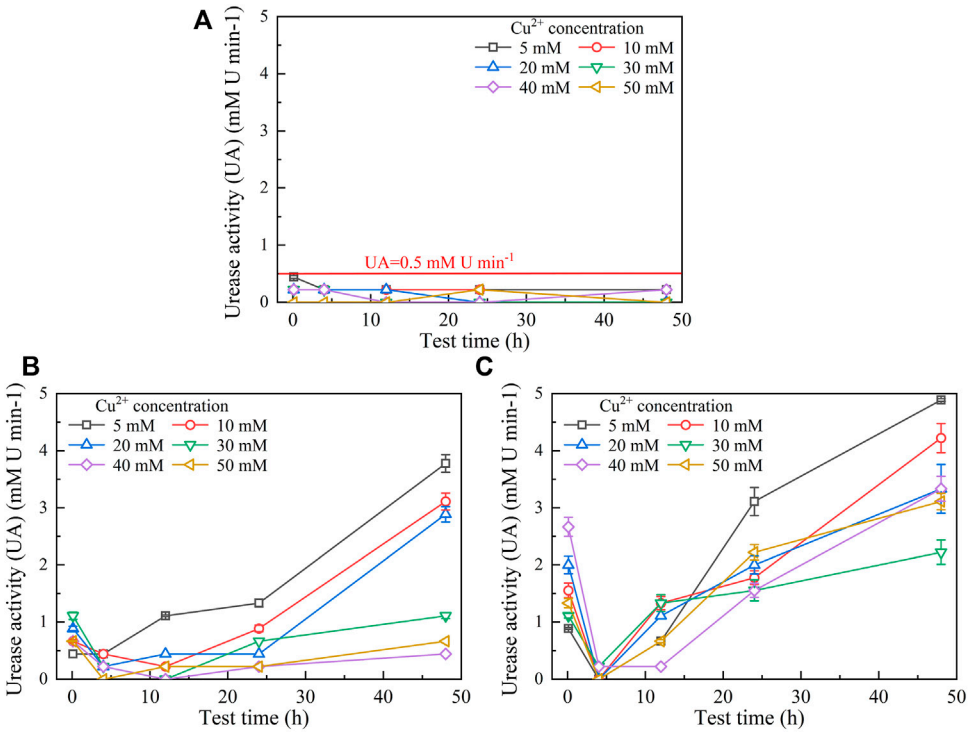

FIGURE 2 | Temporal relationships of pH against $Pb(NO_3)_2$ concentrations: **(A)** without yeast extract and $CaCl_2$, **(B)** under the effect of yeast extract, and **(C)** under the effect of yeast extract and $CaCl_2$ addition.

min^{-1} (maximum) under the effect of Cu^{2+} increases to UA = 13 mM U min^{-1} (maximum) under the effect of Pb^{2+} (**Figures 1**, **3**), indicating the effect of Cu^{2+} on the bacterial activity outweighing the effect of Pb^{2+}. For this reason, UA under the effect of Cu^{2+} could be as low as 0.5 mM U min^{-1} (**Figure 3A**). The effect of Cu^{2+} depresses the ureolytic bacteria and then UA, as indicated by the descending tendency from 0 to 4 h (**Figure 3B**). The effect of yeast extract aids the ureolytic bacteria to secrete urease and promotes notably the development of UA. This especially holds true when subjected to lower Cu^{2+} concentrations and is considered the main cause, leading to a discrepancy in the curve slope after 24 h. As indicated by the measurements of UA, when the ureolytic bacteria provide nucleation sites for precipitating $CaCO_3$, the concentration of the ureolytic bacteria in the supernanant is reduced and the development of UA is depressed, forming the descending tendency from 0 to 4 h (**Figure 3C**). The addition of $CaCl_2$ not only promotes the formation of $CaCO_3$ but also develops resistance of the ureolytic bacteria against the effect of Cu^{2+}. Such resistance is especially significant when subjected to lower Cu^{2+} concentrations, which also indicates the main cause leading to the difference of the curve slope after 4 h. On the other hand, the lower the Cu^{2+} concentration, the higher the degree of urea hydrolysis, and the higher the concentration of NH_4^+ and CO_3^{2-}. The higher concentrations of NH_4^+, induced by Cu^{2+} = 5 mM, turn pH surrounding conditions into a strong alkaline environment (i.e., pH = 9), while due to Cu^{2+} = 50 mM, the lower concentrations of NH_4^+ turn pH surrounding conditions to a weak acid environment (i.e., pH below 6) (**Figure 4A**). The effect of yeast extract differentiates pH under higher Cu^{2+} concentrations from those under lower Cu^{2+} concentrations (**Figure 4B**). There appear two groups; one is pH above 7 and the other is pH below 6. The effect of yeast extract and $CaCl_2$ addition, in turn, eases such difference in pH (**Figure 4C**).

Evaluation of Remediation Efficiency

Figures 5, 6 show the variations of NH_4^+ concentration against Pb^{2+} and Cu^{2+} concentrations, respectively, after 0.1, 24, and 48 h. It is evident that when subjected to no yeast extract and calcium source addition, the higher the concentration of Pb^{2+} or Cu^{2+}, the lower the degree of urea hydrolysis, and the lower the concentration of NH_4^+ (**Figure 5A** and **Figure 6A**). Furthermore, the concentration of NH_4^+ remains nearly unchanged throughout the process, indicating that the majority of the ureolytic bacteria lose their activity when subjected to the effect of Pb^{2+} or Cu^{2+}, and this leads to the inability of discharging NH_4^+ and CO_3^{2-} while catalyzing urea hydrolysis. Under the effect of yeast extract, the concentration of NH_4^+ shows a significant change with time, indicating a continuous discharge of NH_4^+ and CO_3^{2-} (**Figures 5B**, **6B**). This result also indicates that the yeast extract can ease the effect of Pb^{2+} or Cu^{2+} and prevent the ureolytic bacteria from losing their activity. It is worth noting that the more significant change in NH_4^+ concentration under the effect of Pb^{2+} than under the effect of Cu^{2+} provides testimony of the effect of Cu^{2+} outweighing the effect of Pb^{2+}. When the ureolytic bacteria, under

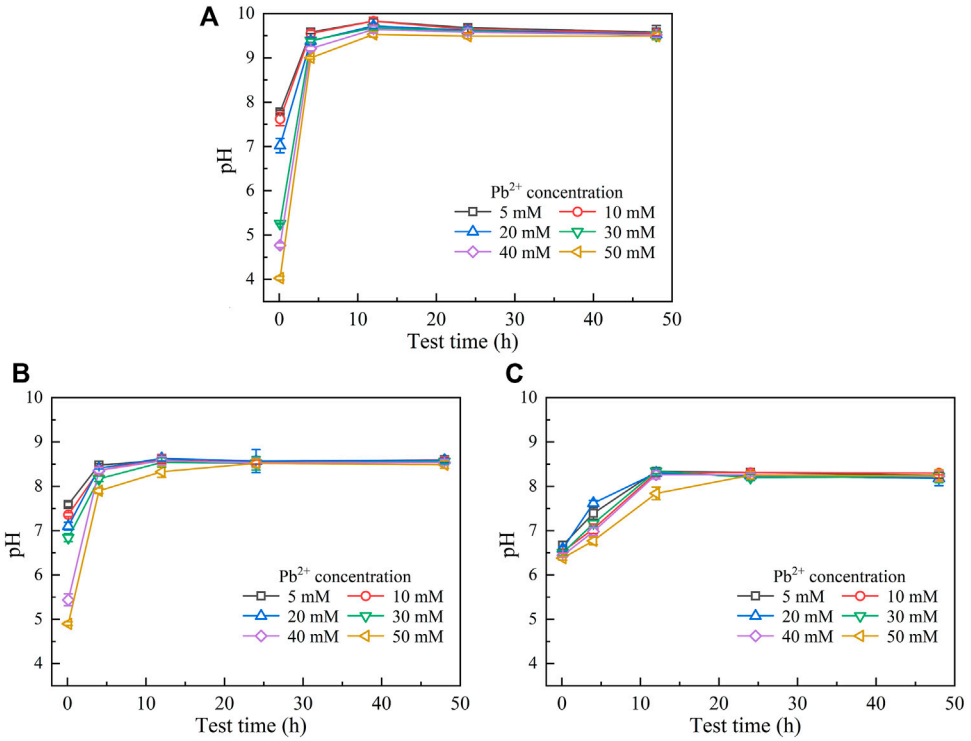

FIGURE 3 | Temporal relationships of urease activity (UA) against $Cu(NO_3)_2$ concentrations: **(A)** without yeast extract and $CaCl_2$, **(B)** under the effect of yeast extract, and **(C)** under the effect of yeast extract and $CaCl_2$ addition.

the effect of yeast extract and $CaCl_2$ addition, start showing their resistance against the effect of Pb^{2+} or Cu^{2+}, the concentration of NH_4^+ after 0.1 h differs notably from that after 24 and 48 h (**Figures 5C**, **6C**); the concentration of NH_4^+, under Pb^{2+} = 5 mM, increases quickly from approximately 110 mM after 0.1 h to about 800 mM after 48 h, while under Cu^{2+} = 5 mM, the concentration of NH_4^+ increases from about 190 mM after 0.1 h to approximately 600 mM after 48 h. Although the addition of $CaCl_2$ promotes the precipitation of $CaCO_3$ and depresses the ureolytic bacteria at the very beginning of the process (i.e., after 0.1 h), it enhances the resistance of the ureolytic bacteria against the effect of Pb^{2+} or Cu^{2+} after 24 and 48 h. This is deemed as the main cause leading to the exaggerated difference between the concentration of NH_4^+ after 0.1 h and the concentration of NH_4^+ after 24 and 48 h.

It is widely known that the lower the remaining heavy metal concentration after catalyzing urea hydrolysis and precipitating carbonate, the higher the remediation efficiency. Figure 7 presents the relationships of the remediation efficiency versus $Pb(NO_3)_2$ concentration after 0.1, 24, and 48 h. The remediation efficiency could be as low as 80% when subjected to no yeast extract and calcium source addition. It is increased to 92% under the effect of yeast extract and further to 100% under the effect of yeast extract and $CaCl_2$ addition. It is worth noting that Pb^{2+} > 20 mM starts depressing the ureolytic bacteria, and therefore, there appears a sudden decline in the remediation efficiency when subjected to no yeast extract and calcium source addition. In contrast, a similar decline cannot be observed when subjected either to the effect of yeast extract or to the effect of yeast extract and $CaCl_2$ addition. On the other hand, for a given concentration of $Pb(NO_3)_2$, the remediation efficiency is increased notably from 0.1 to 24 h, and its increase from 24 to 48 h becomes insignificant as before. These results are especially significant when subjected to no yeast extract and calcium source addition and are in good agreement with the measurements of NH_4^+ concentration, as shown in **Figure 6**. Figure 8 shows the relationships of the remediation efficiency versus $Cu(NO_3)_2$ concentration after 0.1, 24, and 48 h. The remediation efficiency of about 20% is measured when $Cu(NO_3)_2$ concentration = 5 mM, and it sharply increases to higher than 80% when $Cu(NO_3)_2$ concentration = 10 mM (see **Figure 8A**). The remediation efficiency continues to increase to as high as 92% when $Cu(NO_3)_2$ concentration = 30 mM, and then it decreases and remains constant when $Cu(NO_3)_2$ concentration falls in a 40–50 mM range. Under the effect of yeast extract, the remediation efficiency below 10% is measured when $Cu(NO_3)_2$ concentration falls in a 5–10 mM range, and it is increased up to approximately 80% when $Cu(NO_3)_2$ concentration = 50 mM (**Figure 8B**). The remediation efficiency under the effect of yeast extract and $CaCl_2$ addition is measured to be below 10% when $Cu(NO_3)_2$ concentration falls in a 5–30 mM range (**Figure 8C**). It increases to about 77% when $Cu(NO_3)_2$ concentration = 40 mM and further to 84% when $Cu(NO_3)_2$ concentration = 50 mM. These results indicate

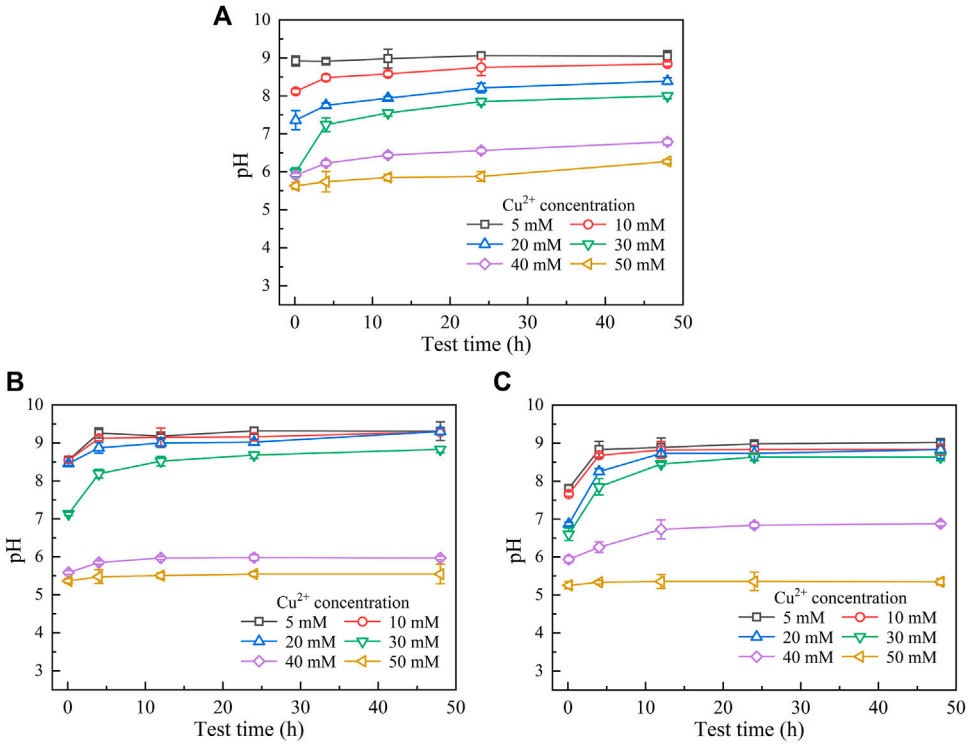

FIGURE 4 | Temporal relationships of pH against $Cu(NO_3)_2$ concentrations: **(A)** without yeast extract and $CaCl_2$, **(B)** under the effect of yeast extract, and **(C)** under the effect of yeast extract and $CaCl_2$ addition.

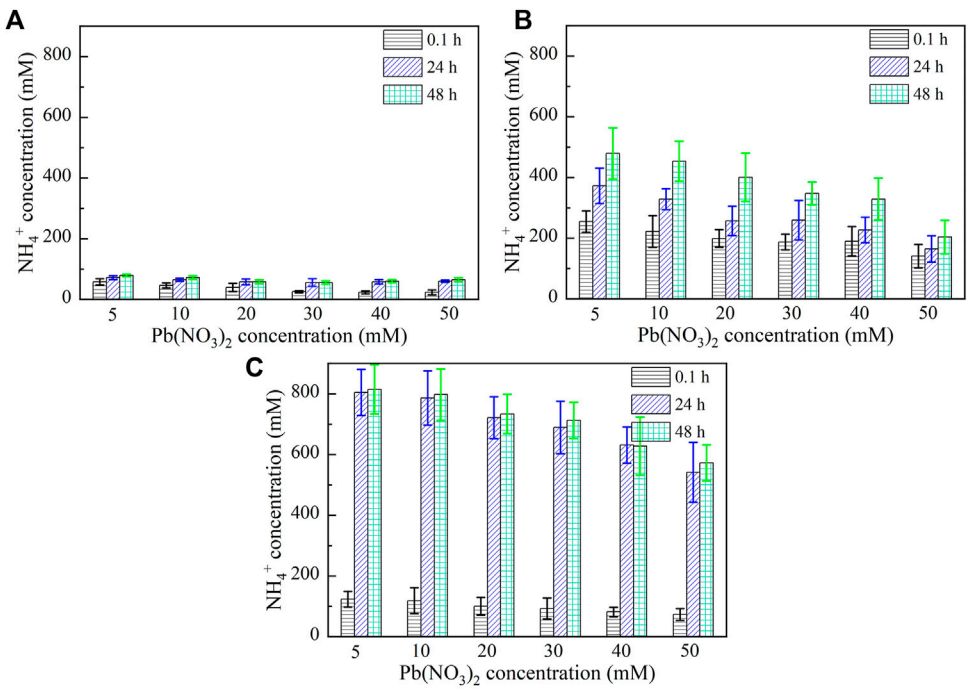

FIGURE 5 | Relationships of NH_4^+ concentration versus $Pb(NO_3)_2$ concentration: **(A)** without yeast extract and $CaCl_2$, **(B)** under the effect of yeast extract, and **(C)** under the effect of yeast extract and $CaCl_2$ addition.

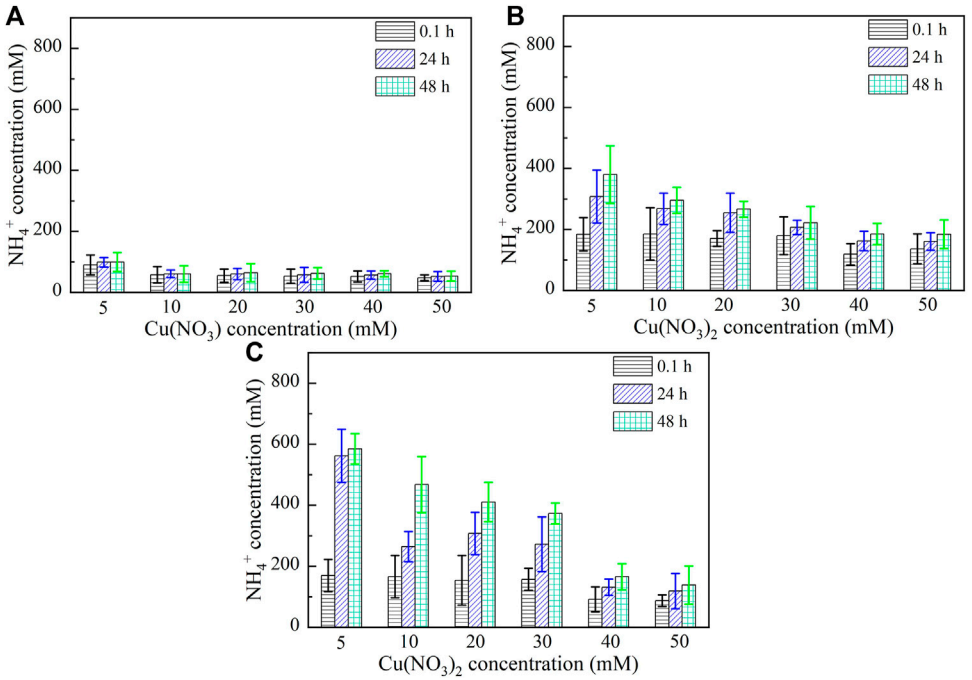

FIGURE 6 | Relationships of NH_4^+ concentration versus $Cu(NO_3)_2$ concentration: **(A)** without yeast extract and $CaCl_2$, **(B)** under the effect of yeast extract, and **(C)** under the effect of yeast extract and $CaCl_2$ addition.

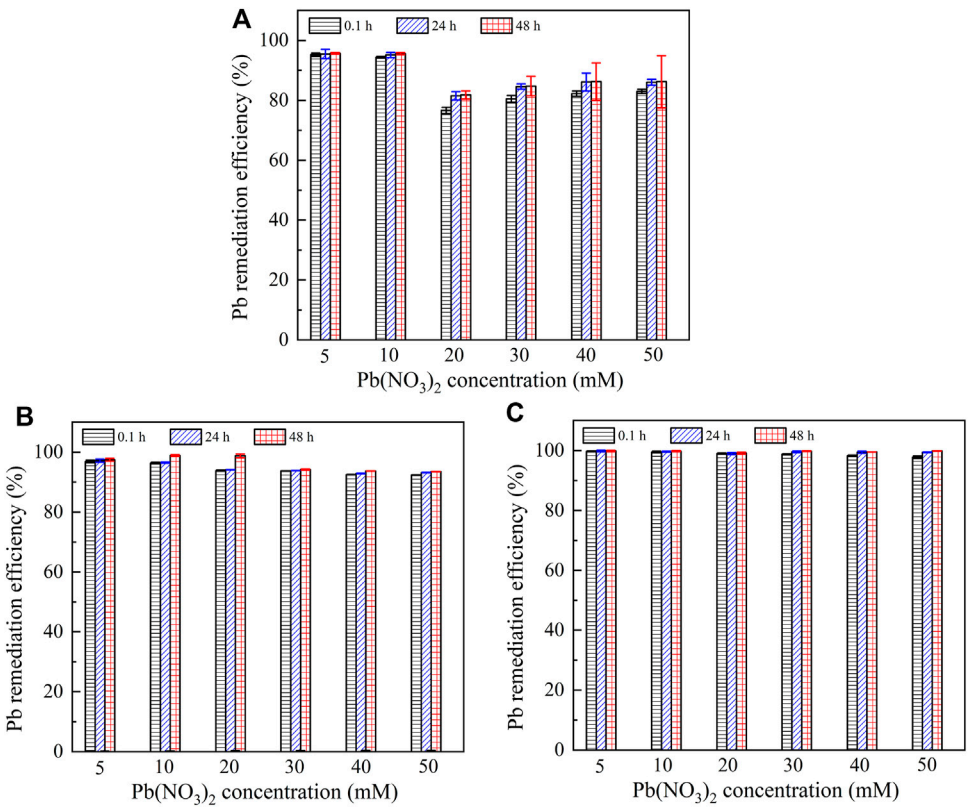

FIGURE 7 | Relationship of remaining Pb^{2+} concentration and Pb remediation efficiency versus $Pb(NO_3)_2$ concentration: **(A)** without yeast extract and $CaCl_2$, **(B)** with yeast extract, and **(C)** with yeast extract and $CaCl_2$.

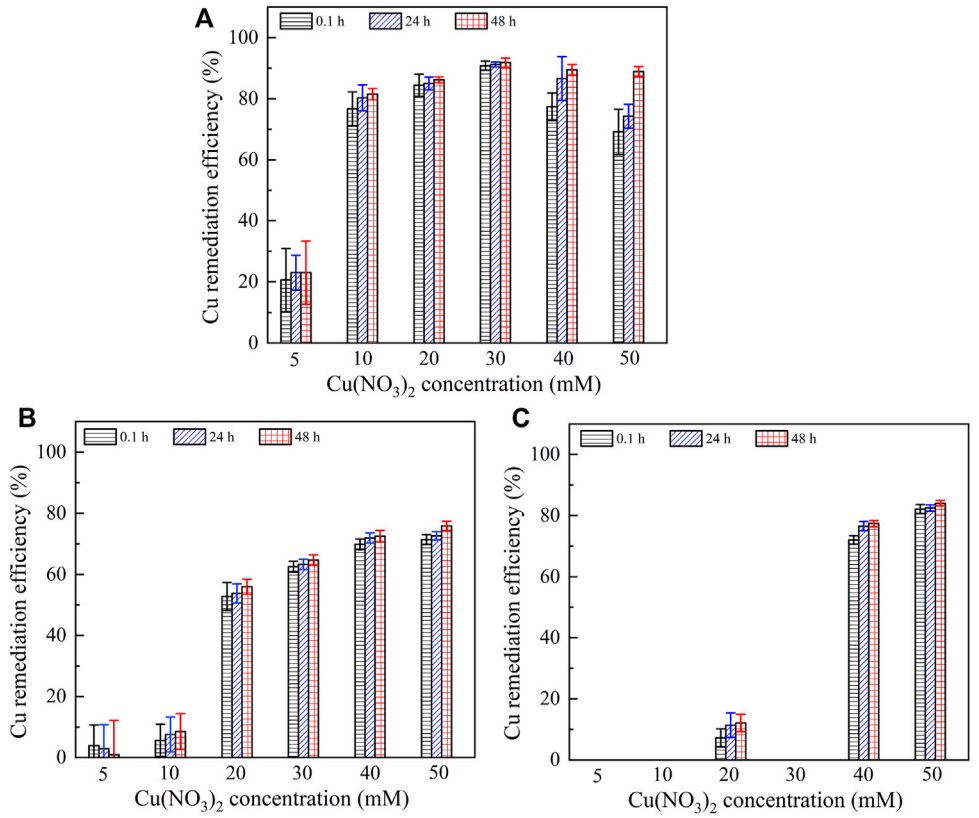

FIGURE 8 | Relationship of remaining Cu^{2+} concentration and Cu remediation efficiency versus $Cu(NO_3)_2$ concentration: **(A)** without yeast extract and $CaCl_2$, **(B)** with yeast extract, and **(C)** with yeast extract and $CaCl_2$.

that the remediation efficiency against Cu^{2+} is not as good as that against Pb^{2+}, and its reduction appears to present in some specific ranges of $Cu(NO_3)_2$ concentration. Further exploration to identify the speciation and sequence of carbonate precipitation is considered of great necessity in order to reveal the mechanisms leading to the reduction in the remediation efficiency. In light of this, biomineralization simulations were conducted in the present work, and the simulated results are presented and analyzed as follows.

Biomineralization Simulation

Carbonate precipitations present in the test tube experiments were simulated by Visual MINTEQ software toward investigating their speciation and sequence of precipitation. NH_4^+ and CO_3^{2-} concentrations that are extracted upon the completion of urea hydrolysis in the test tube experiments are inputted in the biomineralization simulations. Furthermore, when the effect of yeast extract has already increased the degree of urea hydrolysis, the biomineralization simulations were simplified to those considering the effect of calcium source addition only. Figure 9A shows the relationships of the remediation efficiency versus the hydrolyzed urea concentration against $Pb(NO_3)_2$ concentrations varying within a 5–50 mM range, when subjected to no calcium source addition, in which the hydrolyzed urea concentration can be equivalent to the concentration of CO_3^{2-} (i.e., degree of urea hydrolysis). When the hydrolyzed urea concentration is 500 mM, the degree of urea hydrolysis is 100% (**Table 2**). In contrast, the degree of urea hydrolysis corresponds to 0% when the hydrolyzed urea concentration is reduced to 0 mM. Given that the concentration of $Pb(NO_3)_2$ is 10 mM and the speciation of carbonate precipitation is recognized as $Pb_3(CO_3)_2(OH)_2$, 10 mM CO_3^{2-} can precipitate 15 mM Pb^{2+} (= 10 × 3/2), which is in excess of 10 mM Pb^{2+} and also indicates the remediation efficiency being 100% (**Figure 9A**). When the discharge of CO_3^{2-} does not reach a concentration that is required to precipitate Pb^{2+}, the remediation efficiency is degraded where PbCl(OH), $(PbCl)_2CO_3$, and $Pb_3(CO_3)_2(OH)_2$ are precipitated (**Figure 9A**). In contrast, when subjected to the effect of $CaCl_2$ addition, $PbCl_2$, PbCl(OH), $(PbCl)_2CO_3$, and $Pb_3(CO_3)_2(OH)_2$ are precipitated when a lower concentration of the CO_3^{2-} present causes difficulty in precipitating Pb^{2+} (**Figure 9B**). As the concentration of CO_3^{2-} in the biomineralization process is high enough, the speciation of carbonate precipitation corresponds to $PbCO_3$ under no calcium source addition and $PbCO_3$ and $CaCO_3$ under the effect of $CaCl_2$ addition (see **Eqs 6**, **7**). These results show that the speciation of carbonate precipitation varies not only with the concentration of CO_3^{2-} but also with the calcium source addition. **Figure 9C** shows the relationships of the remediation efficiency versus the hydrolyzed urea concentration against

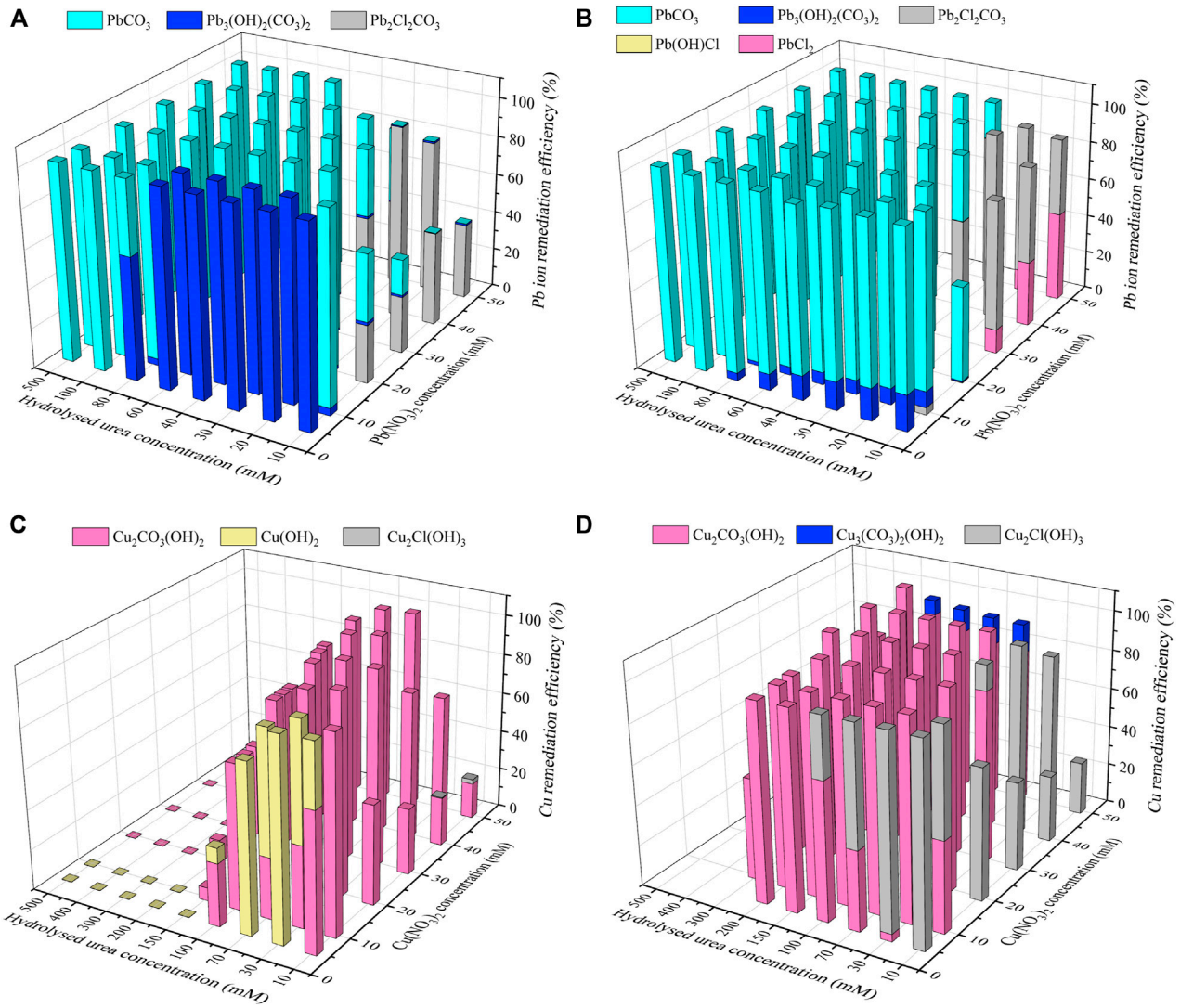

FIGURE 9 | Variations of the Pb remediation efficiency against different Pb^{2+} concentration ranges considering hydrolysed urea concentrations varying in a 10–100 mM: **(A)** no calcium source addition; **(B)** with $CaCl_2$ addition; variations of the Cu remediation efficiency against different Cu^{2+} concentration ranges considering hydrolysed urea concentrations varying in a 10–500 mM: **(C)** no calcium source addition; **(D)** with $CaCl_2$ addition.

$Cu(NO_3)_2$ concentrations varying in a 5–50 mM range, when subjected to no calcium source addition. They behave in an ascending manner in the first place and then in a descending manner, which differs from what we have seen in **Figure 9A**. $Cu_2Cl(OH)_3$ and $Cu_3(CO_3)_2(OH)_2$ are precipitated when low CO_3^{2-} concentration precipitates a small number of Cu^{2+}. In contrast, high CO_3^{2-} precipitates the majority of Cu^{2+}, and $Cu_2CO_3(OH)_2$ is precipitated. $Cu_2Cl(OH)_3$, $Cu_3(CO_3)_2(OH)_2$, and $Cu_2CO_3(OH)_2$, when under the effect of $CaCl_2$ addition, are transformed with the increasing concentration of CO_3^{2-} to $CaCO_3$ (**Figure 9D**). The degradation in the remediation efficiency against Pb^{2+} presents under lower CO_3^{2-} concentrations (corresponding to higher Pb^{2+} concentrations), whereas it vanishes or becomes minimal when subjected to higher CO_3^{2-} concentrations (corresponding to lower Pb^{2+} concentrations) (**Figures 9A,B**). However, the degradation in the remediation efficiency against Cu^{2+} presents not only under lower CO_3^{2-} concentrations but also under higher ones, indicating that it does not rely only on the concentrations of CO_3^{2-} but on other influencing factors. They are worthy of investigation, revealing the mechanism affecting the remediation efficiency against Cu^{2+}. As indicated by the measurements of pH, the higher the degree of urea hydrolysis, the closer the pH surrounding conditions to approximately 9, and the more significant the degradation in the remediation efficiency against Cu^{2+} (**Figure 4B**). In other words, the degradation in the remediation efficiency against Cu^{2+} is also attributed to pH surrounding conditions. However, the degradation in the remediation efficiency, under the effect of $CaCl_2$ addition, appears not as significant as that under no calcium source addition. The effect of $CaCl_2$ addition seems to ease the

impact of pH surrounding conditions because in most cases, the remediation efficiency of approximately 100% is attained when the hydrolyzed urea concentration falls within a 0–300 mM range (corresponding to Cu^{2+} concentration range of 30–50 mM). This is due to the fact that Ca^{2+} which ionized from $CaCl_2$ can react with CO_3^{2-} to form $CaCO_3$ precipitation, where CO_3^{2-} is obtained by the reaction of CO_2 produced by urea hydrolysis with OH^-. A large amount of OH^- is consumed, reducing the pH value of the solution (see **Eqs 1–6**). The reducing pH causes a difficulty in promoting the formation of copper–ammonia complexes.

Mechanisms Affecting Remediation Efficiency

Pb^{2+} or Cu^{2+} can notably affect the ureolytic bacteria and urease activity in the biomineralization process, leading to some difficulty in elevating the degree of urea hydrolysis and attaining a satisfactory remediation efficiency. Generally, the higher the concentration of Pb^{2+} or Cu^{2+}, the lower the degree of urea hydrolysis, and lower the remediation efficiency. Furthermore, the effect of Cu^{2+} outweighing the effect of Pb^{2+} explains why the remediation efficiency against Cu^{2+} is much lower than that against Pb^{2+}. On the other hand, the effect of yeast extract is proven effective in reducing the effect of Pb^{2+} or Cu^{2+} and causing the ureolytic bacteria to secrete urease for catalyzing urea hydrolysis. The experimental results indicate that the degradation in the remediation efficiency against Cu^{2+} is not only counted upon the degree of urea hydrolysis but also upon pH surrounding conditions. In the present work, a pH of approximately 9 leads to the lowest remediation efficiency. In light of this, attaining satisfactory remediation efficiency relies upon the degree of urea hydrolysis and pH surrounding conditions, while remedying Cu^{2+}. When the degree of urea hydrolysis is high enough but the remediation efficiency is not as high as expected, a modification of pH surrounding conditions is considered to be of great necessity. Notwithstanding that, the simulated results indicate that the degradation in the remediation efficiency against Cu^{2+} presents when subjected not only to lower degrees of urea hydrolysis but also to higher degrees of urea hydrolysis. Such a high degree of urea hydrolysis turns pH surrounding conditions into highly alkaline environments, thereby modifying the speciation of carbonate precipitation (i.e. copper–ammonia complexes). The formation of copper–ammonia complexes turns Cu^{2+} into a free state toward degrading the remediation efficiency. The effect of $CaCl_2$ addition eases the degradation in the remediation efficiency. It is worth noting that there appears a discrepancy in the remediation efficiency between the experimental and simulated results, most likely because of the neglection of dissolution of carbonate precipitation by the biomineralization simulations.

On the whole, attaining a satisfactory remediation efficiency relies generally upon the degree of urea hydrolysis. pH surrounding conditions, while remedying Cu^{2+}, can significantly degrade the remediation efficiency. The effect of yeast extract prevents the ureolytic bacteria from losing their activity under heavy metal ion stress. The degradation in the remediation efficiency against Cu^{2+} also presents under higher degrees of urea hydrolysis. This is due to the fact that such a high degree of urea hydrolysis turns pH surrounding conditions into highly alkaline environments, thereby promoting the formation of copper–ammonia complexes and degrading the remediation efficiency. The effect of $CaCl_2$ addition modifies pH surrounding conditions and further eases the degradation in the remediation efficiency. These results shed light on the importance of modifying pH surrounding conditions in capsulizing Cu^{2+} using the bioinspired calcium carbonate precipitation.

CONCLUSION

This study investigated the effects of bacterial culture and calcium source addition on Pb and Cu remediation using the bioinspired calcium carbonate precipitation. Based on the results and discussion, some main conclusions can be drawn as follows:

1) The effect of Cu^{2+} outweighing the effect of Pb^{2+} explains why the remediation efficiency against Cu^{2+} is much lower than that against Pb^{2+}. The lower the degree of urea hydrolysis, the lower the remediation efficiency. The effect of yeast extract reduces the effect of Pb^{2+} or Cu^{2+} on the ureolytic bacteria and urease activity.
2) Ca^{2+} forms competitive adsorption with Pb^{2+} and binds themselves with the ureolytic bacteria, enhancing the resistance against Pb^{2+}. Ca^{2+} play different roles while remedying Cu^{2+}, namely, modifying pH surrounding conditions, preventing the formation of copper–ammonia complexes, and securing the remediation efficiency.
3) The degree of urea hydrolysis might not be the most crucial factor in terms of the remediation efficiency against Cu^{2+}. The findings shed light on the importance of modifying pH in capsulizing Cu^{2+} using the bioinspired calcium carbonate precipitation.

DATA AVAILABILITY STATEMENT

The original contributions presented in the study are included in the article/Supplementary Material, further inquiries can be directed to the corresponding author.

AUTHOR CONTRIBUTIONS

Z-FX: data curation, formal analysis, validation, software, and writing—original draft. W-CC: conceptualization, methodology, writing—review and editing, supervision, and funding acquisition. LW: writing—review and editing. SW: writing—review and editing.

FUNDING

This study is based upon work supported by the Shaanxi Educational Department under Grant No. 2020TD-005 through the innovative ability support scheme.

REFERENCES

Achal, V., Pan, X., and Zhang, D. (2012). Bioremediation of Strontium (Sr) Contaminated Aquifer Quartz Sand Based on Carbonate Precipitation Induced by Sr Resistant Halomonas Sp. *Chemosphere* 89, 764–768. doi:10.1016/j.chemosphere.2012.06.064

Arias, D., Cisternas, L. A., Miranda, C., and Rivas, M. (2019). Bioprospecting of Ureolytic Bacteria from Laguna Salada for Biomineralization Applications. *Front. Bioeng. Biotechnol.* 6, 209. doi:10.3389/fbioe.2018.00209

Bai, B., Xu, T., Nie, Q., and Li, P. (2020). Temperature-driven Migration of Heavy Metal Pb2+ along with Moisture Movement in Unsaturated Soils. *Int. J. Heat Mass Transfer* 153, 119573. doi:10.1016/j.ijheatmasstransfer.2020.119573

Bai, X. D., Cheng, W. C., Ong, D. E. L., and Li, G. (2021a). Evaluation of Geological Conditions and Clogging of Tunneling Using Machine Learning. *Geomechanics Eng.* 25 (1), 59–73. doi:10.12989/gae.2021.25.1.059

Bai, X.-D., Cheng, W.-C., Sheil, B. B., and Li, G. (2021b). Pipejacking Clogging Detection in Soft Alluvial Deposits Using Machine Learning Algorithms. *Tunnelling Underground Space Tech.* 113, 103908. doi:10.1016/j.tust.2021.103908

Bai, B., Nie, Q., Zhang, Y., Wang, X., and Hu, W. (2021c). Cotransport of Heavy Metals and SiO2 Particles at Different Temperatures by Seepage. *J. Hydrol.* 597, 125771. doi:10.1016/j.jhydrol.2020.125771

Bai, X. D., and Cheng, W. C. (2021d). A Comparative Study of Different Machine Learning Algorithms in Predicting EPB Shield Behavior: A Case Study at Xi'an Metro, China. *Acta Geotech.* 16 (12), 4061–4080. doi:10.1007/s11440-021-01383-7

Bhattacharya, A., Naik, S. N., and Khare, S. K. (2018). Harnessing the Bio-Mineralization Ability of Urease Producing *Serratia marcescens* and *Enterobacter cloacae* EMB19 for Remediation of Heavy Metal Cadmium (II). *J. Environ. Manage.* 215, 143–152. doi:10.1016/j.jenvman.2018.03.055

Bolan, N., Kunhikrishnan, A., Thangarajan, R., Kumpiene, J., Park, J., Makino, T., et al. (2014). Remediation of Heavy Metal(loid)s Contaminated Soils - to Mobilize or to Immobilize? *J. Hazard. Mater.* 266 (15), 141–166. doi:10.1016/j.jhazmat.2013.12.018

Chen, L., Beiyuan, J., Hu, W., Zhang, Z., Duan, C., Cui, Q., et al. (2022). Phytoremediation of Potentially Toxic Elements (PTEs) Contaminated Soils Using Alfalfa (Medicago Sativa L.): A Comprehensive Review. *Chemosphere* 293, 133577. doi:10.1016/j.chemosphere.2022.133577

Cheng, W. C., Duan, Z., Xue, Z. F., and Wang, L. (2021). Sandbox Modelling of Interactions of Landslide Deposit with Terrace Sediments Aided by Field Observation. *B. Eng. Geol. Environ.* 80, 3711–3731. doi:10.1007/s10064-021-02144-2

Duarte-Nass, C., Rebolledo, K., Valenzuela, T., Kopp, M., Jeison, D., Rivas, M., et al. (2020). Application of Microbe-Induced Carbonate Precipitation for Copper Removal from Copper-Enriched Waters: Challenges to Future Industrial Application. *J. Environ. Manage.* 256, 109938. doi:10.1016/j.jenvman.2019.109938

Gat, D., Ronen, Z., and Tsesarsky, M. (2017). Long-term Sustainability of Microbial-Induced CaCO3 Precipitation in Aqueous media. *Chemosphere* 184, 524–531. doi:10.1016/j.chemosphere.2017.06.015

Hu, W. L., Cheng, W. C., Wen, S. J., and Yuan, K. (2021). Revealing the Enhancement and Degradation Mechanisms Affecting the Performance of Carbonate Precipitation in EICP Process. *Front. Bioeng. Biotechnol.* 9, 750258. doi:10.3389/fbioe.2021.750258

Hu, W., Cheng, W.-C., Wen, S., and Mizanur Rahman, M. (2021a). Effects of Chemical Contamination on Microscale Structural Characteristics of Intact Loess and Resultant Macroscale Mechanical Properties. *Catena* 203, 105361. doi:10.1016/j.catena.2021.105361

Hu, W., Cheng, W.-C., Wen, S., and Yuan, K. (2021b). Revealing the Enhancement and Degradation Mechanisms Affecting the Performance of Carbonate Precipitation in EICP Process. *Front. Bioeng. Biotechnol.* 9, 750258. doi:10.3389/fbioe.2021.750258

Hu, W. L., Cheng, W. C., Wang, L., and Xue, Z. F. (2022). Micro-Structural Characteristics Deterioration of Intact Loess Under Acid and Saline Solutions and Resultant Macro-Mechanical Properties. *Soil Tillage Res.* 220, 105382. doi:10.1016/j.still.2022.105382

Jiang, N.-J., Liu, R., Du, Y.-J., and Bi, Y.-Z. (2019). Microbial Induced Carbonate Precipitation for Immobilizing Pb Contaminants: Toxic Effects on Bacterial Activity and Immobilization Efficiency. *Sci. Total Environ.* 672, 722–731. doi:10.1016/j.scitotenv.2019.03.294

Jimenez-Lopez, C., Jroundi, F., Pascolini, C., Rodriguez-Navarro, C., Pinar-Larrubia, G., and Rodriguez-Gallego, M. (2008). Consolidation of Quarry Calcarenite by Calcium Carbonate Precipitation Induced by Bacteria Activated Among the Microbiota Inhabiting the Stone. *Int. Biodeterior. Biodegrad.* 62, 352–363. doi:10.1016/j.ibiod.2008.03.002

Khadim, H. J., Ammar, S. H., and Ebrahim, S. E. (2019). Biomineralization Based Remediation of Cadmium and Nickel Contaminated Wastewater by Ureolytic Bacteria Isolated from Barn Horses Soil. *Environ. Tech. Innovation* 14, 100315. doi:10.1016/j.eti.2019.100315

Li, M., Cheng, X., and Guo, H. (2013). Heavy Metal Removal by Biomineralization of Urease Producing Bacteria Isolated from Soil. *Int. Biodeterioration Biodegradation* 76, 81–85. doi:10.1016/j.ibiod.2012.06.016

Liao, P., Li, B., Xie, L., Bai, X., Qiao, H., Li, Q., et al. (2020). Immobilization of Cr(VI) on Engineered Silicate Nanoparticles: Microscopic Mechanisms and Site Energy Distribution. *J. Hazard. Mater.* 383, 121145. doi:10.1016/j.jhazmat.2019.121145

Mugwar, A. J., and Harbottle, M. J. (2016). Toxicity Effects on Metal Sequestration by Microbially-Induced Carbonate Precipitation. *J. Hazard. Mater.* 314, 237–248. doi:10.1016/j.jhazmat.2016.04.039

Nakata, H., Nakayama, S., Oroszlany, B., Ikenaka, Y., Mizukawa, H., Tanaka, K., et al. (2017). Monitoring lead (Pb) Pollution and Identifying Pb Pollution Sources in Japan Using Stable Pb Isotope Analysis with Kidneys of Wild Rats. *Int. J. Environ. Res. Public Health* 14 (1), 56–69. doi:10.3390/ijerph14010056

Omoregie, A. I., Khoshdelnezamiha, G., Senian, N., Ong, D. E. L., and Nissom, P. M. (2017). Experimental Optimisation of Various Cultural Conditions on Urease Activity for Isolated Sporosarcina Pasteurii Strains and Evaluation of Their Biocement Potentials. *Ecol. Eng.* 109, 65–75. doi:10.1016/j.ecoleng.2017.09.012

Peng, Y., Zhang, S., Zhong, Q., Wang, G., Feng, C., Xu, X., et al. (2021). Removal of Heavy Metals from Abandoned Smelter Contaminated Soil with Poly-Phosphonic Acid: Two-Objective Optimization Based on Washing Efficiency and Risk Assessment. *Chem. Eng. J.* 421, 129882. doi:10.1016/j.cej.2021.129882

Qiao, R. J., Shao, Z. S., Liu, F. Y., and Wei, W. (2019). Damage Evolution and Safety Assessment of Tunnel Lining Subjected to Long Duration Fire. *Tunnelling and Underground Space Technology* 83, 354–363. doi:10.1016/j.tust.2018.09.036

Qiao, S., Zeng, G., Wang, X., Dai, C., Sheng, M., Chen, Q., et al. (2021). Multiple Heavy Metals Immobilization Based on Microbially Induced Carbonate Precipitation by Ureolytic Bacteria and the Precipitation Patterns Exploration. *Chemosphere* 274 (8), 129661. doi:10.1016/j.chemosphere.2021.129661

Rahman, M. M., Hora, N. R., Ahenkorah, I., Beecham, S., Karim, M. R., and Iqbal, A. (2020). State-of-the-art Review of Microbial-Induced Calcite Precipitation and its Sustainability in Engineering Applications. *Sustainability* 12 (15), 1–43. doi:10.3390/su12156281

Rajasekar, A., Wilkinson, S., and Moy, C. K. S. (2021). MICP as a Potential Sustainable Technique to Treat or Entrap Contaminants in the Natural Environment: A Review. *Environ. Sci. Ecotechnology* 6, 100096. doi:10.1016/j.ese.2021.100096

Rui Zhang, R., Wu, K., Jiang, Z. W., and Wang, J. Y. (2021). Bacterially Induced $CaCO_3$ Precipitation for the Enhancement of Quality of Coal Gangue. *Construction Building Mater.* 319, 126102. doi:10.1016/j.cej.2021.129723

Schwantes-Cezario, N., Medeiros, L. P., De Oliveira, A. G., Jr, Nakazato, G., Katsuko Takayama Kobayashi, R., and Toralles, B. M. (2017). Bioprecipitation of Calcium Carbonate Induced by Bacillus Subtilis Isolated in Brazil. *Int. Biodeterioration Biodegradation* 123, 200–205. doi:10.1016/j.ibiod.2017.06.021

Schwantes-Cezario, N., Ferreira Nogueira Camargo, G. S., Franco do Couto, Á., Porto, M. F., Cremasco, L. V., Andrello, A. C., et al. (2020). Mortars with the Addition of Bacterial Spores: Evaluation of Porosity Using Different Test Methods. *J. Building Eng.* 30, 101235. doi:10.1016/j.jobe.2020.101235

Seplveda, S., Duarte-Nass, C., Rivas, M., Azcar, L., Ramrez, A., Toledo-Alarcn, J., et al. (2021). Testing the Capacity of Staphylococcus Equorum for Calcium and Copper Removal through MICP Process. *Minerals* 11, 905. doi:10.3390/min11080905

Shi, T., Xie, Z., Zhu, Z., Shi, W., Liu, Y., and Liu, M. (2022). Highly Efficient and Selective Adsorption of Heavy Metal Ions by Hydrazide-Modified Sodium Alginate. *Carbohydr. Polym.* 276, 118797. doi:10.1016/j.carbpol.2021.118797

Song, H., Wang, C., Kumar, A., Ding, Y., Li, S., Bai, X., et al. (2021). Removal of Pb2+ and Cd2+ from Contaminated Water Using Novel Microbial Material (Scoria@UF1). *J. Environ. Chem. Eng.* 9, 106495. doi:10.1016/j.jece.2021.106495

Stocks-Fischer, S., Galinat, J. K., and Bang, S. S. (1999). Microbiological Precipitation of CaCO3. *Soil Biol. Biochem.* 31, 1563–1571. doi:10.1016/s0038-0717(99)00082-6

Teng, Z., Shao, W., Zhang, K., Huo, Y., and Li, M. (2019). Characterization of Phosphate Solubilizing Bacteria Isolated from Heavy Metal Contaminated Soils and Their Potential for lead Immobilization. *J. Environ. Manage.* 231, 189–197. doi:10.1016/j.jenvman.2018.10.012

Torres-Aravena, Á., Duarte-Nass, C., Azócar, L., Mella-Herrera, R., Rivas, M., and Jeison, D. (2018). Can Microbially Induced Calcite Precipitation (MICP) through a Ureolytic Pathway Be Successfully Applied for Removing Heavy Metals from Wastewaters? *Crystals* 8, 438. doi:10.3390/cryst8110438

Vital, B., Bartacek, J., Ortega-Bravo, J. C., and Jeison, D. (2018). Treatment of Acid Mine Drainage by Forward Osmosis: Heavy Metal Rejection and Reverse Flux of Draw Solution Constituents. *Chem. Eng. J.* 332, 85–91. doi:10.1016/j.cej.2017.09.034

Wang, J.-F., Li, W.-L., Ahmad, I., He, B.-Y., Wang, L.-L., He, T., et al. (2021). Biomineralization of Cd2+ and Inhibition on Rhizobacterial Cd Mobilization Function by Bacillus Cereus to Improve Safety of maize Grains. *Chemosphere* 283, 131095. doi:10.1016/j.chemosphere.2021.131095

Wang, L., Cheng, W. C., Xue, Z. F., and Hu, W. L. (2022). Effects of the Urease Concentration and Calcium Source on Enzyme-Induced Carbonate Precipitation for Lead Remediation.. *Front. Chem.* 10, 892090. doi:10.3389/fchem.2022.892090

Wang, L., Cheng, W. C., and Xue, Z. F. (2022). Investigating Microscale Structural Characteristics and Resultant Macroscale Mechanical Properties of Loess Exposed to Alkaline and Saline Environments. *B. Eng. Geol. Environ.* 81, 146. doi:10.1007/s10064-022-02640-z

Wang, L., Cheng, W.-C., and Xue, Z.-F. (2022). The Effect of Calcium Source on Pb and Cu Remediation Using Enzyme-Induced Carbonate Precipitation. *Front. Bioeng. Biotechnol.* 10, 849631. doi:10.3389/fbioe.2022.849631

Whiffin, V. S., van Paassen, L. A., and Harkes, M. P. (2007). Microbial Carbonate Precipitation as a Soil Improvement Technique. *Geomicrobiology J.* 24, 417–423. doi:10.1080/01490450701436505

Wu, M., Li, Y., Li, J., Wang, Y., Xu, H., and Zhao, Y. (2019). Bioreduction of Hexavalent Chromium Using a Novel Strain CRB-7 Immobilized on Multiple Materials. *J. Hazard. Mater.* 368, 412–420. doi:10.1016/j.jhazmat.2019.01.059

Xue, Z.-F., Cheng, W.-C., Wang, L., and Song, G. (2021a). Improvement of the Shearing Behaviour of Loess Using Recycled Straw Fiber Reinforcement. *KSCE J. Civ Eng.* 25 (9), 3319–3335. doi:10.1007/s12205-021-2263-3

Xue, Z. F., Cheng, W. C., and Wang, L. (2021b). Effect of Straw Reinforcement on the Shearing and Creep Behaviours of Quaternary Loess. *Sci. Rep.* 11 (1), 19926. doi:10.1038/s41598-021-99318-5

Xue, Z.-F., Cheng, W.-C., Wang, L., and Hu, W. (2022). Effects of Bacterial Inoculation and Calcium Source on Microbial-Induced Carbonate Precipitation for lead Remediation. *J. Hazard. Mater.* 426, 128090. doi:10.1016/j.jhazmat.2021.128090

Yang, T., Li, Y., Hong, Y., Chi, L., Liu, C., Lan, Y., et al. (2020). The Construction of Biomimetic Cementum through a Combination of Bioskiving and Fluorine-Containing Biomineralization. *Front. Bioeng. Biotechnol.* 8, 341. doi:10.3389/fbioe.2020.00341

Yang, Y., Reddy, K. R., Zhan, H., Fan, R., Liu, S., Xue, Q., et al. (2021). Hydraulic Conductivity of Soil-Bentonite Backfill Comprised of SHMP-Amended Ca-Bentonite to Cr(VI)-impacted Groundwater. *J. contaminant Hydrol.* 242, 103856. doi:10.1016/j.jconhyd.2021.103856

Yin, T., Lin, H., Dong, Y., Li, B., He, Y., Liu, C., et al. (2021). A Novel Constructed Carbonate-Mineralized Functional Bacterial Consortium for High-Efficiency Cadmium Biomineralization. *J. Hazard. Mater.* 401, 123269. doi:10.1016/j.jhazmat.2020.123269

Yuan, Y., Shao, X. S., Qiao, R. J., Fei, X. S., Cheng, J. X., and Wei, W. (2021). Fracture behavior of concrete coarse aggregates under microwave irradiation influenced by mineral components. *Constr. Build. Mater.* 286, 122944. doi:10.1016/j.conbuildmat.2021.122944

Yuyang Zhang, Y., Zhu, Z., Liao, Y., Dang, Z., and Guo, C. (2021). Effects of Fe(II) Source on the Formation and Reduction Rate of Biosynthetic Mackinawite: Biosynthesis Process and Removal of Cr(VI). *Chem. Eng. J.* 421, 129723. doi:10.1016/j.cej.2021.129723

Zhao, M., Xu, Y., Zhang, C., Rong, H., and Zeng, G. (2016). New Trends in Removing Heavy Metals from Wastewater. *Appl. Microbiol. Biotechnol.* 100, 6509–6518. doi:10.1007/s00253-016-7646-x

Zhao, W.-W., Zhu, G., Daugulis, A. J., Chen, Q., Ma, H.-Y., Zheng, P., et al. (2020). Removal and Biomineralization of Pb2+ in Water by Fungus Phanerochaete Chrysoporium. *J. Clean. Prod.* 260, 120980. doi:10.1016/j.jclepro.2020.120980

Zhu, T. J., and Maria, D. S. (2016). Carbonate Precipitation Through Microbial Activities in Natural Environment, and Their Potential in Biotechnology: A Review. *Front. Bioeng. Biotechnol.* 4, 1–21. doi:10.3389/fbioe.2016.00004

Conflict of Interest: The authors declare that the research was conducted in the absence of any commercial or financial relationships that could be construed as a potential conflict of interest.

Publisher's Note: All claims expressed in this article are solely those of the authors and do not necessarily represent those of their affiliated organizations, or those of the publisher, the editors, and the reviewers. Any product that may be evaluated in this article, or claim that may be made by its manufacturer, is not guaranteed or endorsed by the publisher.